Colloids and Surfaces B: Biointerfaces 184 (2019) 110544

Contents lists available at ScienceDirect

Colloids and Surfaces B: Biointerfaces

journal homepage: www.elsevier.com/locate/colsurfb

Stereocomplexed PLA microspheres: Control over morphology, drug encapsulation and anticancer activity

M. Brzeziński[a,*], B. Kost[a], S. Wedepohl[b], M. Socka[a], T. Biela[a], M. Calderón[b,c,d]

[a] Centre of Molecular and Macromolecular Studies, Polish Academy of Sciences, Sienkiewicza 112, 90-363 Lodz, Poland
[b] Freie Universität Berlin, Institute of Chemistry and Biochemistry, Takustr. 3, 14195 Berlin, Germany
[c] POLYMAT and Applied Chemistry Department, Faculty of Chemistry, University of the Basque Country UPV/EHU, Paseo Manuel de Lardizabal 3, 20018 Donostia-San Sebastián, Spain
[d] IKERBASQUE, Basque Foundation for Science, 48013 Bilbao, Spain

ARTICLE INFO

Keywords:
Stereocomplex microspheres
Morphology and size control
Drug delivery systems
Anticancer activity

ABSTRACT

Lung cancer is the leading cause of cancer death because of smoking and air pollution. Therefore, new ideas should be provided for lung cancer treatment in which the delivery of anticancer drugs to the local tumor site can be achieved. For this purpose, we propose the use of stereocomplexed spherical microspheres with sizes between 0.5 and 10 μm loaded with doxorubicin (DOX) to be administered through the nasal route. In order to gain control over the microsphere morphology, size, and drug loading capacity, we systematically studied the influence of the solvent used for preparation and the functionalization of their building blocks, namely poly-L-lactide (PLLA) and poly-D-lactide (PDLA) with blocked or unblocked L-proline moieties. We could demonstrate that DOX release is generally determined by the size of the microspheres. The antiproliferative activity of DOX released from the different microspheres was shown *in vitro* using the A549 lung cancer cell line as a model. Moreover, when in direct contact to the cancer cells, smaller microspheres were uptaken and could serve as a reservoir for local drug release. Our findings not only provide a novel strategy to prepare PLA microspheres with controllable morphology and release of anti-cancer drugs but also offer additional possibilities for the application of stereocomplexed particles in anticancer therapy, with suitable sizes for nasal administration.

1. Introduction

Polylactide (PLA) is exploited as a biocompatible polymer matrix for drug support in various biomedical applications [1–3]. In comparison to materials solely composed of homocrystallites of poly(L-lactide) (PLLA) or poly(D-lactide) (PDLA), the formation of stereocomplexes (sc-PLA) between the equimolar mixture of PLLA and PDLA enhance the hydrolysis resistance, thermal, and mechanical properties of sc-PLA materials [4–6]. These differences allow for designing of PLA-based materials with controllable thermal stability, mechanical properties or biodegradation [7–9]. Moreover, the mixing of PLLA and PDLA enantiomers in the proper organic solvents induces the formation of stereocomplexed microspheres [10–12]. For their application as drug delivery systems (DDS), it is crucial to obtain control over their size, morphology, and porosity [8,13–15]. Recently, it was reported that the dynamic interactions between vanillin versus imine chain end modified PLLA and PDLA during the stereocomplex formation allows for the control of the nanostructure morphology through reversible amine-imine transformation [5]. However, there have been no reports of the introduction of amino acid end groups into PLA to control the size, morphology and drug release from stereocomplexed microspheres. Therefore, we have introduced L-proline functionality to PLA backbone because we assumed such functionality could be implemented as a targeting moiety and enhanced anti-tumor efficiency of microparticles [16], as it was demonstrated for amino acid functionalized prodrugs against melanoma [17], cervical [18], and breast cancer [19].

Moreover, it has been shown for poly(lactide-co-glycolide) (PLGA) microspheres, that the drug loading efficiency could be adjusted by the type and the composition of organic solvents used for their preparation [20]. Stereocomplexed PLA-based microspheres are typically prepared in a single solvent, such as acetonitrile [12], tetrahydrofuran (THF) [21] or 1,4-dioxane (DIOX) [22]. It is possible to assume that by the dissolution of PLLA/PDLA in the binary mixture of these two solvents in different ratios, it should be possible to additionally tune the particles crystallinity [23] and encapsulation efficiency [20].

In this work, we propose to functionalize PLLA and PLDA with

* Corresponding author.
E-mail address: mbrzezin@cbmm.lodz.pl (M. Brzeziński).

https://doi.org/10.1016/j.colsurfb.2019.110544
Received 1 June 2019; Received in revised form 10 September 2019; Accepted 2 October 2019
Available online 09 October 2019

blocked or unblocked L-proline moieties in order to modulate the interactions occurring between the polymer chains, while they precipitate from mixture of organic solvents. To introduce amino acid end groups, hydroxyl-Boc-L-proline was used as an initiator of both L-LA and D-LA polymerization, and subsequently, this end group was deprotected to yield L-proline functionalized PLAs. Such polymeric building blocks were subsequently used for the preparation of doxorubicin (DOX) containing stereocomplexed microparticles. We hypothesize that by modulation of PLA end group functionality, namely, Boc-protected L-proline versus unblocked L-proline PLAs, we should be able to control the self-assembly of the polymeric building blocks [24], modulate the morphology, and the drug release from stereocomplexed microspheres. As a proof of concept, we performed DOX release experiments at physiological conditions (pH 7.4) to probe if the size and morphology of obtained stereocomplexed microspheres influence the DOX release. Moreover, we investigated the efficiency of DOX-loaded microparticles against A549 cell lines to analyse if the different size of microspheres play a role in their antiproliferative activity. To the best of our knowledge, this represents the first report on the development of stereocomplexed microspheres based on PLAs with l-proline moieties as efficient anti-cancer microcarrier.

2. Experimental section

2.1. Materials

Tin (II) octoate (2-ethylhexanoate) $Sn(Oct)_2$ (commercial product from Sigma-Aldrich) was purified by two consecutive high-vacuum distillations at 140 °C/3 × 10^{-3} mbar. The purified $Sn(Oct)_2$, stored on the vacuum line, was finally directly distributed into thin-walled vials or ampules equipped with break-seals and then sealed off and stored at −12 °C. l,L-lactide and d,D-lactide (99%, Purac, Netherlands) were consecutively crystallized from dry 2-propanol and purified just before use by sublimation *in vacuo* (10^{-3} mbar, 85 °C). Tetrahydrofuran (THF, POCH, Gliwice, Poland, 99%) was kept for several days over KOH pellets, filtered off, and refluxed over Na metal. Eventually, it was distilled, degassed, and stored over a liquid Na/K alloy, and it developed a blue color. Methanol (POCH, Gliwice, Poland, pure p.a. grade), 1,4-dioxane (Sigma Aldrich), DOX·HCl (Sigma Aldrich), N-Boc-trans-4-hydroxy-L-proline methyl ester (Sigma Aldrich), phosphate buffer saline (PBS) pH 7.4 (Sigma Aldrich), Trifluoroacetic acid (Sigma Aldrich) were used as received. As a cell culture medium for A549 cells, DMEM supplemented with 10% FBS (Merck Millipore) and 1% Penicillin/Streptomycin (Thermo Fisher Scientific) was used.

2.2. Ring-opening of L- and D-lactide

The linear PLLA and PDLA enantiomeric polymers were synthesized according to a well-established procedure [22]. l,L-lactide or d,D-lactide (5.70 g, 40 mmol) was polymerized in THF at 80 °C with $Sn(Oct)_2$ (1 mL of 0.25 mol L^{-1} solution in dry THF) and N-Boc-trans-4-hydroxy-L-proline methyl ester (0.6 g, 2.36 mmol) as components of the catalytic/initiating system. The resulting polymer was dissolved in $CHCl_3$ and precipitated into methanol, separated by filtration and washed several times with methanol. Boc-LP-PLA − OH, ^{1}H NMR ($CDCl_3$): 5.35 (br s, 1H, L-proline end group), 5.14 (1H, q, polymer), 4.31 (1H, q, end group polymer) and (1H, t, L-proline end group), (1H, 3.8-3.6 (2H, m, L-proline end group), 3.47 (3H, s, $-OCH_3$ in L-proline end group) 2.33 (2H, m, L-proline end group), 2.2 (2H, m, L-proline end group), 1.47 (3H, d, polymer) 1.39–1.45 (Boc-protecting group).

2.3. Unblocking of L-proline functionalized PLAs

Deprotection of the Boc-protecting group was done as previously described [24]. Briefly, polymer ester (0.5 g, 0.1 mmol) was dissolved in CH_2Cl_2, and trifluoroacetic acid (TFA) was added. With vigorous stirring, the process was conducted for 24 h. Subsequently, the PLLA or PDLA was precipitated into a large excess of methanol, resulting in a white powder. LP-PLA − OH, ^{1}H NMR ($CDCl_3$): 5.35 (br s, 1H, L-proline end group), 5.14 (1H, q, polymer), 4.31 (1H, q, end group polymer) and (1H, t, L-proline end group), (1H, 3.8-3.6 (2H, m, L-proline end group), 2.55 (2H, m, L-proline end group), 2.4 (2H, m, L-proline end group), 1.47 (3H, d, polymer).

2.4. Preparation of blank and DOX-loaded microparticles

Stereocomplex formation was carried out as follows: 50 mg of Boc-L-proline/L-proline PLLA and 50 mg of Boc-L-proline/L-proline PDLA were dissolved separately in 1 mL of DIOX, THF or in their binary mixtures with different proportions of both solvents, then the solutions were mixed together and (after short stirring) left at room temperature without stirring. The initially clear mixture became turbid after ~1–2 h. After ~24 h the supernatant was removed by decantation, the solid was washed with three portions (1 mL each) of fresh DIOX (or THF) and dried at room temperature under a slight vacuum. The same procedure was used for the DOX-loaded stereocomplexed microparticles in which for each enantiomer 50 μL of DOX solution in DMSO was added.

2.5. Encapsulation efficiency

For the determination of drug loading content, the DOX-loaded NPs solution was lyophilized and then dissolved in DMSO. The amount of the encapsulated DOX was estimated by fluorescence spectroscopy (λ = 590 nm) according to a calibration curve. Encapsulation efficiency (EE%) was calculated according to the following formula:

$$EE\% = (W_t/W_i) \times 100\%$$

Where W_t is the theoretical amount of drug loaded in microparticles and W_i is actual amount of drug loaded in microparticles.

2.6. In vitro drug release

To determine the release profile from stereocomplexed microspheres composed of PLLA and PDLA with blocked and un-blocked L-proline end groups were loaded with DOX. Then, 1.5 mg of these microspheres were suspended in 1.5 mL of PBS buffer solutions in 2-mL centrifuge tubes and incubated at 37 °C. At determined intervals, the tubes were centrifuged at 6000 rpm for 5 min using a Galaxy Ministar microcentrifuge, and the supernatant was collected and replaced by an equal volume of fresh buffer solution. The amount of released drug in the supernatant was quantified from fluorescence emission spectra measured on a Fluorog-3 (Horiba Jobin-Yvon) fluorimeter. The emission of the DOX was observed in the range of 590 nm upon excitation with UV light of 490 nm. The percentage of DOX release at each time was calculated by normalizing the data to the total amount of drug in particles.

2.7. Cell viability assay

A549 cells (#ACC-107, Leibnitz Institute DSMZ – German Collection of Microorganisms and Cell Cultures) were seeded into 96 well plates in DMEM (Thermo Fisher Scientific) with 10% FBS (biowest) 1% penicillin/streptomycin (Thermo Fisher Scientific) and grown over night at 37 °C and 5% CO_2. Dry microspheres were weighed and transferred to 2 mL microcentrifuge tubes. Particles were suspended in medium to a final concentration of 1 mg/mL and incubated at 37 °C. After 2 h, 6 h and 24 h, 4 × 100 μL of each tube were removed and added to the cells to 100 μL/well. Cells were incubated for 48 h with the conditioned medium (extracts from the particles). Then, the supernatant was removed and replaced with 100 μL/well fresh medium containing 10 μL/

well MTT (5 mg/mL in PBS, Sigma). After 4 h of incubation at 37 °C, the supernatant was removed and replaced with isopropanol containing 0.04 M HCl. Absorbance was read in a Tecan M200Pro microplate reader at 570 nm. Absorbance from wells without cells were subtracted. Relative viability was calculated as absorbance values of treated cells divided by absorbance values of untreated cells and expressed as %.

2.8. Confocal laser scanning microscopy

A549 cells were seeded into 8-well μ-slides (ibidi) and grown over night at 37 °C and 5% CO_2. On the next day, a small amount of the dry particles was added as a powder using a spatula and incubated for 24 h at 37 °C and 5% CO_2. After the incubation time, cells were washed 5x with PBS to remove all loose particles and fresh medium containing Hoechst 33342 (Sigma) to stain the nuclei was added. Cells were imaged live using a Leica SP8 confocal laser scanning microscope and images were acquired using LASX software (Leica). Emitted DOX fluorescence was collected from 569 nm to 690 nm (red channel, excitation wavelength 561 nm). As the third channel (blue), Hoechst fluorescence was collected from 413 nm to 485 nm (excitation 405 nm).

2.9. Characterization

^{1}H NMR spectra were recorded in chloroform-d_1 and 1,1,2,2-tetrachloroethane-d_2 on a Bruker DRX500 spectrometer operating at 500 MHz. Traces of the nondeuterated chloroform was used as an internal standard. The number-average molecular weights M_n of the polymers were determined by size exclusion chromatography (SEC) using an Agilent Pump 1100 Series (preceded by an Agilent G1379A Degasser), equipped with a set of two PLGel 5 μ MIXED-C columns. A Wyatt Optilab Rex differential refractometer and a Dawn Eos (Wyatt Technology Corporation) laser photometer were used as detectors. Dichloromethane was used as eluent at a flow rate of 0.8 mL min^{-1} at room temperature. Differential scanning calorimetry (DSC) analysis was performed under nitrogen at a heating and cooling rate of 10 °C/min on a DSC 2920 modulated TA Instruments. Both the temperature and heat flow were calibrated with indium. Fourier-transform infrared spectroscopy (FTIR) spectra were measured with a Nicolet 6700 spectrometer equipped with a deuterated triglycine sulfate (DGTS) detector. Attenuated total reflectance (ATR) was used for IR measurements. The spectra were obtained by adding 64 scans at a 2 cm^{-1} resolution. Scanning electron microscopy (SEM) images were obtained with a Nova Nano SEM 230 instrument (FEI company) equipped with SE Detector at HV = 15 kV and low vacuum (0.3 Torr) with high resolution in lens detector Helix (resolution approximately 2 nm). The samples were prepared by fixing onto carbon adhesive tape and covering with a conductive gold layer, and studied in low vacuum. The electron micrographs were recorded with a resolution of 1024 × 768 pixels.

3. Results and discussion

3.1. Microsphere preparation from L-proline functionalized PLLA/PDLA

Fig. 1 illustrates the synthesis of L-proline functionalized PLLA and PDLA, the unblocking of L-proline end groups and the process of the formation of microspheres from obtained enantiomeric PLAs. The main concept relies on controlling the release of DOX from sc-PLA microspheres prepared by mixing PLLA/PDLA with different end group functionalities in two solvents in variable ratios (THF/DIOX). Towards this aim, low molecular-weight PLLA and PDLA functionalized with L-proline were synthesized by coordination polymerization [25] using hydroxyl-functionalized, Boc-protected L-proline as an initiator of the polymerization process. The single chromatographic peak in the range of 2000–5000 g/mol and the relatively low dispersity ($Đ$ < 1.3-1.4), respectively, indicate the good control over the polymerization process. Macromolecular structure of synthesized PLAs was verified by ^{1}H NMR and MALDI-TOF (Figs. S1 and S2). Unblocking of the amine and carboxylic acid from Boc and ^{t}Bu protecting groups can be readily conducted under acidic conditions. Thus, the obtained PLLAs and PDLAs were deprotected in dry CH_2Cl_2 in the presence of trifluoroacetic acid (TFA) to afford the PLAs with unblocked L-proline end groups. Successful deprotection of both PLLA and PDLA enantiomers was confirmed by comparing appropriate signals of the ^{1}H NMR spectra given in Fig. 1B. The Boc protecting group signals disappeared following deprotection, causing a simplification in the 1.2–1.4 ppm region, and disappearance of methyl group signal at 3.47 ppm. Moreover, the characteristic L-proline end groups signals of CH_2 protons were now shifted from 2.2 to 2.33 and 2.4 to 2.55 ppm, respectively.

Subsequently, stereocomplexed microspheres were formed by spontaneous precipitation of equimolar mixtures of PLLA and PDLA from the solution of THF and 1,4-dioxane and their binary mixtures. The ratios of THF and DIOX were selected as 10:0, 9:1, 7:3, 6:4, 5:5, 4:6, 3:7, 1:9, and 0:10. Equimolar mixtures of blocked/un-blocked L-proline functionalized PLAs in chosen single solvent or mixture of organic solvents (with or without DOX) were kept in this solution at ambient temperature until precipitation occurred. After spontaneous precipitation, the solvent was removed and the obtained microparticles were dried at vacuum and ATR-FTIR analysis was used to confirm the presence of stereocomplex assemblies. As expected, a new band appears in the spectrum of sc-PLA at 909 cm^{-1} derived from skeletal vibrations of the β-helix (characteristic for stereocomplex), whereas the band characteristic for enantiomeric α-helix (921 cm^{-1}) completely disappears [26], as shown in Figure S3.

3.2. Thermal properties of l-proline functionalized PLLA/PDLA microspheres

To provide further proof of stereocomplexation, DSC was used to investigate the thermal properties of stereocomplexed PLAs functionalized with both blocked and un-blocked L-proline end groups. Exemplary DSC traces of the enantiomeric components and stereocomplexed microspheres before/after encapsulation of DOX are summarized in Table S1-S4. Interestingly, the melting temperature of polymeric components after deprotection is slightly higher by ~4 °C than the PLAs with Boc-protected end groups. This observation can possibly indicate that supramolecular interactions between the unblocked L-proline end groups of PLAs enhanced the melting temperature and crystallinity of obtained polymers [27]. Upon blending of obtained PLLA and PDLA, the crystallinity and melting temperature of resulting materials increases by ~50–60 °C relative to that of the individual components [13]. The T_m values of obtained stereocomplexed PLAs are in the range of ~198–209 °C in the first and second heating run of DSC, which is much higher than that of homocrystallites of enantiomeric PLAs (~135–145 °C). The T_m and ΔH_m values of the stereocomplexes obtained via spontaneous precipitation from un-blocked l-proline PLAs are higher in comparison to those with blocked L-proline end groups, as shown in Fig. 2B/D and Table S1/Table S3. It is clear that the three different interactions are possible between L-proline end-capped macromolecules, namely hydrogen bonding, acid-base, and oppositely charge ionic interactions [28]. These supramolecular bondings play an important role in controlling their self-assembly [29] and enhance their crystallization ability [10]. Apart from the influence of the functionality of obtained PLAs on the crystallinity, these values can be tuned by varying ratio of THF and DIOX used for their precipitation. The highest crystallinity is observed for the stereocomplexes prepared in DIOX and lowest for those precipitating from THF. There is also a clear trend in which the crystallinity decreases upon addition THF to DIOX, however only until a certain level (as shown in Table S1 and S3). Moreover, melting peaks at temperatures characteristic for stereocomplexes were observed in the first and second heating runs of DSC, therefore it can be concluded that the stereocomplex formation is fully reversible [30]. The question arose how the addition of DOX would affect the

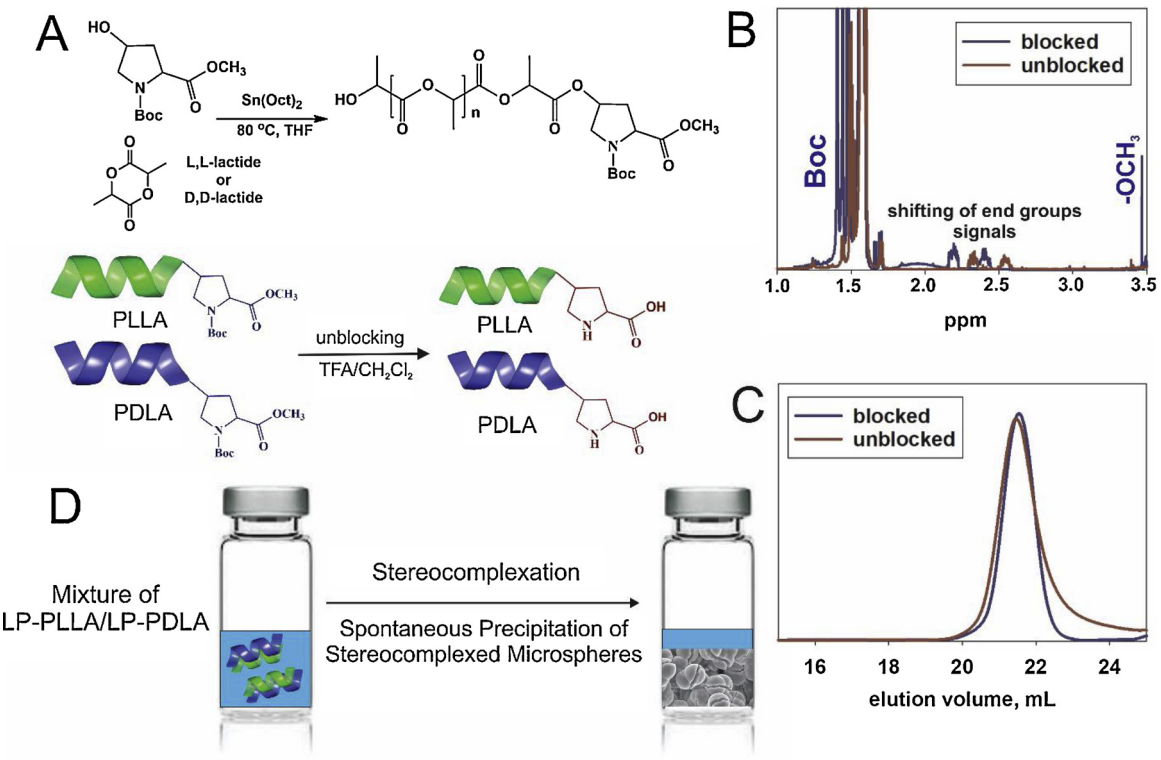

Fig. 1. (A) Synthesis of Boc-L-proline functionalized PLAs and unblocking of the proline end groups, (B) ^{1}H NMR spectra of PLAs before and after unblocking and (C) SEC chromatograms of these PLAs. (D) Scheme of formation of sc-PLA microspheres from enantiomeric PLAs by spontaneous precipitation from solution.

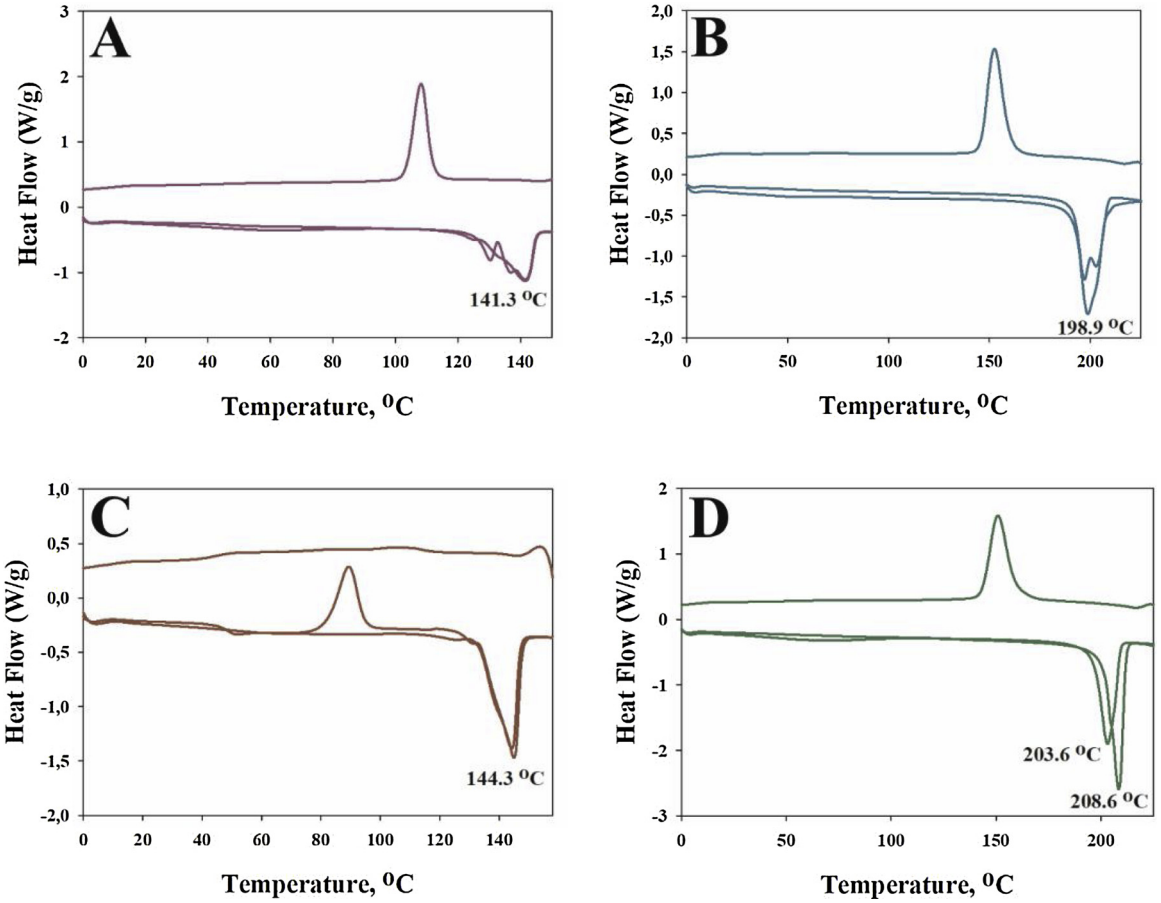

Fig. 2. DSC thermograms of (A) Boc-L-proline and (C) L-proline functionalized PLAs and their stereocomplexes composed of PLAs with (B) blocked and (D) unblocked proline end groups (the values for all samples are presented in Table S1-S4).

stereocomplexation process and morphology of PLA particles during the spontaneous precipitation of microspheres. For the microparticles composed of PLAs with Boc-L-proline end groups, solely stereocomplex crystallites are present in the first and second heating run of DSC and a slight decrease of their crystallinity is observed after DOX encapsulation. Whereas stereocomplexes of PLLA and PDLA without Boc-protected end groups prepared from THF and its mixture with DIOX exhibit the formation of stereocomplex crystallites in the first heating run with only a small fraction of homocrystallities. However, in the second heating run of DSC, only signals characteristic for stereocomplexes are observed. This indicates that more perfect sc-PLA crystals are formed from the melt. The stereocomplexes composed of unblocked PLAs also exhibit lower crystallinity and melting temperatures after addition of DOX.

3.3. Morphological characterization of blank and DOX-loaded L-proline functionalized PLLA/PDLA microspheres

Stereocomplexed microspheres composed of blocked/un-blocked L-proline functionalized PLAs were prepared through spontaneous precipitation in THF, DIOX or in their mixture with different ratios. In our previous work, we have shown that the enantiomeric PLAs self-assembled into stereocomplexed microspheres in THF, whereas a worm-like stereocomplexed nanostructure was formed in DIOX [21]. Therefore, we anticipate that the different solvation of PLLA/PDLA macromolecules in the pure solvents and their binary mixtures would additionally alter the morphology of obtained microparticles. The morphology of the microspheres was characterized in detail by scanning electron microscopy (SEM). After mixing of Boc-L-proline end-capped PLLA and PDLA, three distinct morphologies were observed depending on the solvent used for their preparation. Using THF, porous microspheres with cracks are formed, whereas in DIOX, enantiomeric PLAs self-assemble in the form of pac-man particles, and in the mixture of the two solvents (THF/DIOX: 1:9) uniform microparticles with apparent cracks on the surface are created, as shown in the Fig. 3. Further increase in the THF content does not significantly change the morphology of the uniform microspheres, except for the ratio 3:7, in which ruptures on the surfaces of microspheres were observed (Figure S4). The size of microspheres ranges from 5 to 10 μm, depending on the method of preparation. Since there was only a slight difference in morphology of microspheres after increasing the amount of THF in a binary mixture of THF and DIOX, three formulations were used for the preparation of DOX-loaded microspheres with different ratio of THF and DIOX (10:0, 1:9, 0:10). The particles transform into regular particles after DOX encapsulation, in which small nanometer-sized pores are present as shown in Figure S5. This could be attributed to the presence of DOX which could influence the PLLA and PDLA self-assembly and especially the hydrogen-bonds formation between enantiomeric PLAs [31]. In addition, DOX encapsulation may have also an influence on the surface structure of resulting microparticles [32,33]. Evaporation-driven connective assembly in colloids is controlled by the inter-particle potentials, which is influenced by the surface charge of particles and surrounding media [34]. Therefore, a probable explanation for the different morphology of the particles is the contribution of the DOX in forming competitive hydrogen bonds with PLA macromolecules.

When the L-proline end groups in the PLA microspheres were unblocked, their morphology and size was significantly different from microspheres containing PLAs with blocked end-groups (Fig. 4). Especially, the size of microparticles was lower after deprotection of PLA end-groups and it was in the range 0.5 to 3 μm. We assume that the hydrogen bonding interactions between PLA end groups allow for the pre-organization of macromolecules in the first stage of their self-assembly [22]. Such interactions were impossible in the case of PLAs with Boc-L-proline end groups. Subsequently, during stereocomplexation smaller particles are formed due to combination of cooperative interactions of the enantiomeric PLA segments, as it was shown in previous studies [10,35]. Ajiro et. al. observed that reversible transition imine-vaniline transformation of PLA end-groups allows for the control over the morphology of obtained materials [5]. This was attributed to the difference of hydrophobic-hydrophilic balance after end group deprotection. We assume that our amino acid functionalized PLAs can behave similarly and that the L-proline end groups are able to form hydrogen bonds, allowing for the nanostructure organization of sc-PLA nanoparticles with sizes of about 30 nm which are the building blocks of resulting microspheres [36]. Their size is significantly lower than those with Boc-protected groups due to the extensive interactions of the end-groups [21]. The size of particles prepared without DOX is quite similar to blank microparticles and their size is in the range of 0.5 to 1.5 μm. However, the size of microspheres prepared solely in DIOX after DOX encapsulation is increased to about 3 μm whereas for those prepared in the other solvent combination does not noticeably differ. Moreover, porous pac-man like particles are formed exclusively in DIOX. Therefore, it can be concluded that this kind of morphology is preferred in DIOX, probably due to the solvation of polymers in this solvent which influences the hydrogen-bond interactions between macromolecules and their self-assembly [21]. After DOX encapsulation, the difference in morphology is not as pronounced for THF and its binary mixture as for the Boc-protected PLAs which is in agreement with the work of Pack et. al. for PLGA/PLA microspheres in which the morphology depends on the DOX distribution in the microspheres [33].

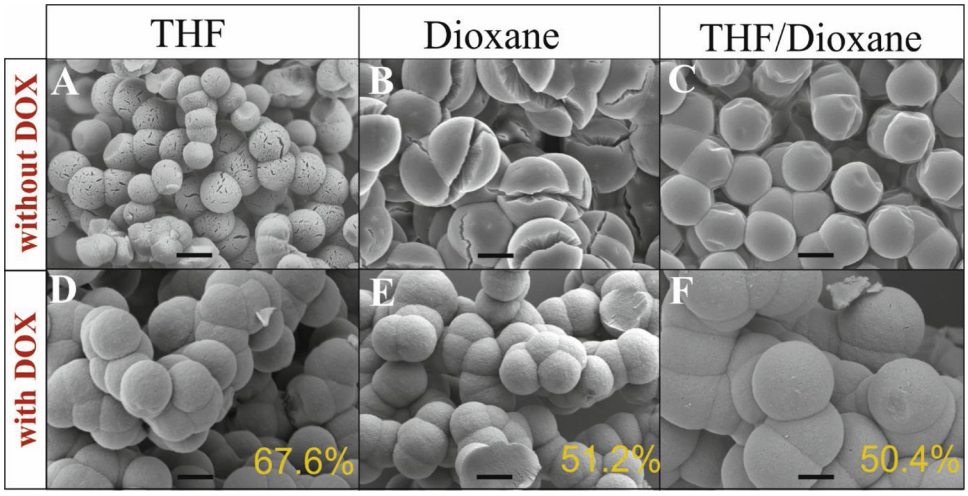

Fig. 3. (A–C) Morphology of the stereocomplexed microspheres composed of Boc-protected L-proline functionalized PLAs prepared in THF, DIOX and their 9:1 binary mixture and (D–F) their DOX-loaded counterparts. The yellow numbers denote the respective DOX encapsulation efficiency (%). The scale bar denotes 5 μm. (For interpretation of the references to colour in this figure legend, the reader is referred to the web version of this article).

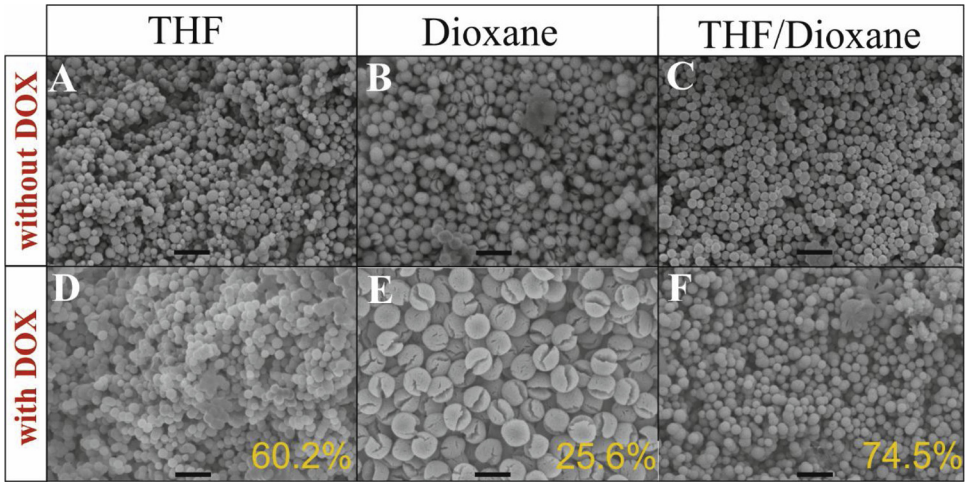

Fig. 4. (A–C) Morphology of the stereocomplexed microspheres composed of unblocked L-proline functionalized PLAs prepared in THF, DIOX and their 9:1 binary mixture and (D–F) their DOX-loaded counterparts. The yellow numbers denote the respective DOX encapsulation efficiency (%). The scale bar denotes 5 μm. (For interpretation of the references to colour in this figure legend, the reader is referred to the web version of this article).

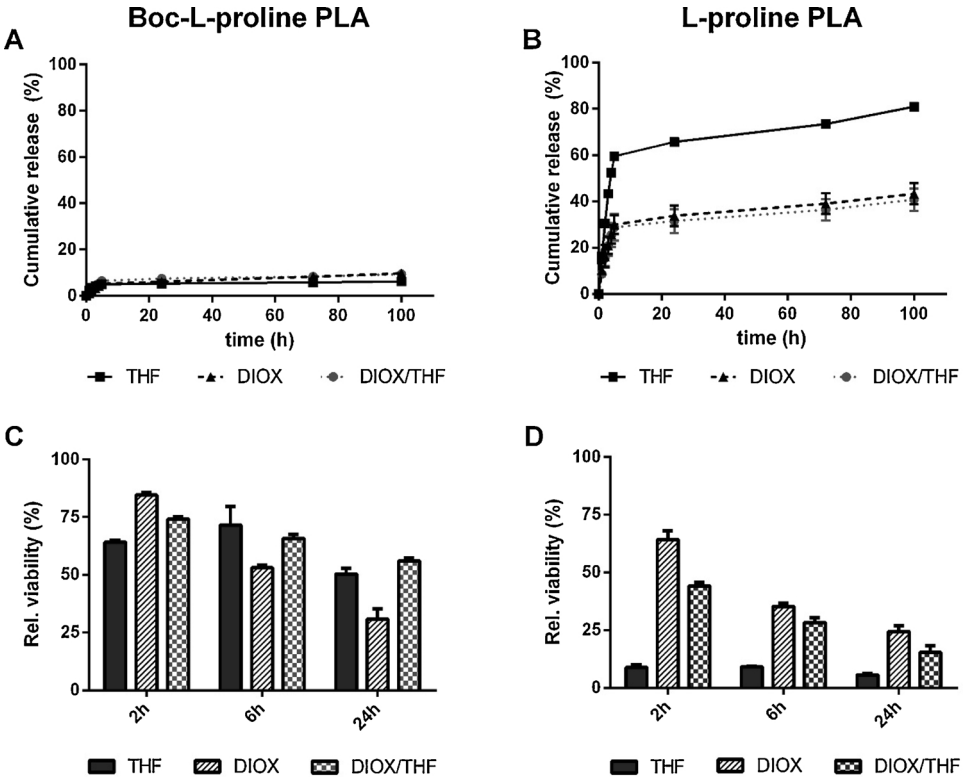

Fig. 5. *In vitro* release profiles of DOX from stereocomplexed microspheres composed of PLLA and PDLA functionalized with (A) Boc-L-proline and (B) L-proline. Antiproliferative activity of medium extracts of DOX-loaded stereocomplexed microspheres composed of (C) Boc-L-proline PLLA/PDLA and (D) L-proline PLLA/PDLA after different incubation times in medium to A459 cells after 48 h, as determined by MTT test.

3.4. Encapsulation and in vitro drug release of L-proline functionalized PLLA/PDLA microspheres

The effect of the different formulations of L-proline functionalized PLLA/PDLA microspheres was investigated in terms of encapsulation efficiency of DOX. All results are summarized in Table S5 and S6 and given in Fig. 5. The encapsulation efficiency (EE) of DOX in microspheres composed of Boc-protected l-proline PLAs was in the range of 50–68% and is highest for the microparticles prepared in THF. In contrary, the situation is totally different for unblocked L-proline PLAs in comparison to blocked ones for which DIOX gives the lowest value of encapsulation efficiency (26%) whereas for THF the EE reaches a value of 60%. In the binary mixture of these two solvents in which the ratio of the THF/DIOX was 9:1, the value is slightly higher (~75%) so even the addition of such small amounts of THF can significantly enhance this value for microspheres from L-proline PLAs. Subsequently, the release of DOX from prepared microspheres was investigated in PBS at 37 °C. The release of drug from microspheres composed of Boc-protected PLLA/PDLA is relatively slow and ranging from 5 to 10% after 100 h, as shown in Fig. 5A. The difference between various formulations is relatively low, however, the release was faster for particles prepared with DIOX and its binary mixture. This can be attributed to the low specific surface of particles and slow hydrolysis rate of microparticles [33]. However, the release from microspheres built from PLLA and PDLA with un-blocked l-proline end groups is completely different and a much faster and higher release of DOX ranging from 41 to 81% is observed, as shown in the Fig. 5B. In the first 6 h, there is an initial burst release and subsequently, DOX is released slowly over a period of ~ 100 h. However, the fastest release is observed for particles prepared in THF, followed by those from the binary mixture of THF/DIOX and in DIOX alone. We ascribe this phenomenon to the presumable difference in drug accumulation in the microspheres composed of Boc-L-proline PLAs versus L-proline PLAs and thus the drug may be released faster from the microspheres composed of L-proline PLAs because it is located

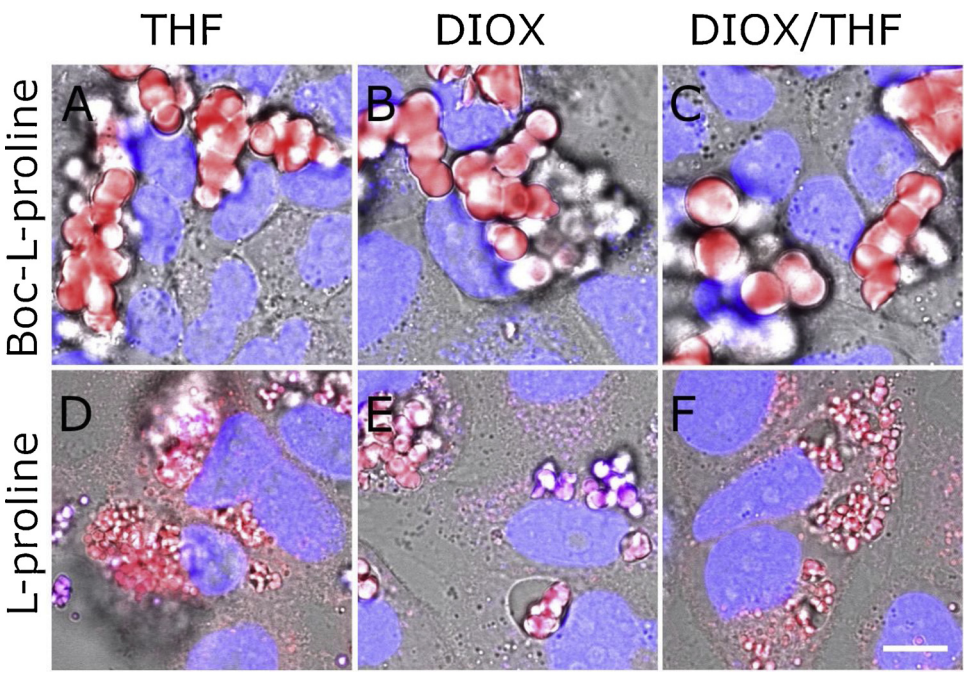

Fig. 6. Confocal laser scanning microscopy images of live A549 cells after 24 h of incubation with the differently formulated DOX loaded microspheres. Boc-L-proline PLA microspheres prepared in (A) THF, (B) DIOX, (C) DIOX/THF and (D–F) their unblocked L-proline PLA counterparts. Merged color images of transmitted light (grey), DOX fluorescence (red) and Hoechst 33342 stained cell nuclei (blue). Scale bar = 10 μm. (For interpretation of the references to colour in this figure legend, the reader is referred to the web version of this article).

near the surface and initial burst release is observed [33,37]. As it was described by Ito et. al. the release of the drugs depends on the distribution of the drug on the surface or in the interior of the particle [20]. Therefore, the preparation method and PLAs used (with blocked versus un-blocked end groups) allow to optimize the release from obtained sc-PLAs microparticles due to the size of microparticles, the drug distribution in their interior, and in the lower extent from morphology.

3.5. Anti-cancer effects of drug loaded PLLA/PDLA microspheres

In order to assess the cytotoxicity of stereocomplexed DOX-containing microspheres *in vitro*, the viability of A459 cells incubated with medium extracts of the obtained microspheres was evaluated using MTT assay. After incubation of 1 mg/mL of microparticles for 2 h at 37 °C, there was a slight reduction in cell viability, which was however not increased after prolonged exposure times of 6 h to 24 h, as shown in Figure S6. To test the cell proliferation inhibition activity of DOX delivered by the loaded stereocomplexed microparticles, A459 cells were treated with medium extracts of Boc-protected L-proline and L-proline functionalized PLLA/PDLA microspheres for 2, 6 and 24 h. The time-dependent increase in cytotoxicity mediated by conditioned media confirmed that functional DOX is successfully released to the medium over time causing its concentration-dependent specific reduction in cell viability. However, there is a marked difference between the set of particles prepared from Boc-protected L-proline and L-proline functionalized PLLAs/PDLAs, mainly due to the different size of microparticles and the rate of DOX release. Moreover, the cell viability also differs with the solvent used for the preparation of microparticles which determines their structure and size. For the microspheres composed of Boc-protected PLLA/PDLA, the highest antiproliferative activity was observed for the particles prepared in DIOX, however, due to the slow release of the DOX, complete cell death is not achieved over the course of the experiment, as shown in Fig. 5C. This could be overcome by applying the microparticles composed of unblocked L-proline functionalized PLLAs/PDLAs for which high anti-cancer activity is observed, as shown in Fig. 5D. This is correlated with the release profiles in which the high amount of DOX is released during the 24 h of incubation in PBS. However, the highest efficiency in killing cancer cells was observed for the particles prepared in THF, followed by those from the binary mixture of THF and DIOX and finally from 1,4-dioxane. This shows the high influence of the size and morphology of obtained DOX-loaded stereocomplexed microspheres for drug delivery to lung cancer cells. Thus, it could be hypothesized that the optimal preparation conditions and polymer functionalities determined the amount of delivering DOX to lung cancer cells and the efficiency of the potential therapy.

To investigate the effect of the microsphere morphology on cells in direct contact, we incubated the different DOX-loaded formulations for 24 h on A549 cells and observed them by confocal microscopy (Fig. 6 and Figures S8-S12). We can clearly see the DOX fluorescence associated with the particles and the sizes and shapes similar to the ones observed by SEM. The microspheres prepared from Boc-L-proline PLAs were partly associated with the cells, leaving them however largely unaffected (Fig. 6 A–C) consistent with the results from our cell viability study. The smaller microspheres resulting from unblocked L-proline PLAs however were uptaken by the cells and hence found within their cytoplasm. It is well known that cellular uptake of microparticles is size dependent [38], which is reflected here. Although free DOX is usually found in the cell nucleus after diffusing into cells, we did not observe clear DOX fluorescence in the nuclei for all formulations. However, the cytotoxic effect of DOX is clearly seen on the cells treated with the unblocked L-proline PLA microspheres (Fig. 6D–F) by their disturbed cellular morphology such as membrane blebs and vacuolization as well as detachment and lower cell density in the monolayer. We propose that the particles can act as reservoirs for slow and steady drug release closely associated or within the cells, but in this experiment, the intracellular concentration of released DOX is not high enough to be detected with the microscope. Consistent with the previously presented results, the therapeutic effect of DOX on lung cancer cells appears to be largest when delivered by the unblocked L-proline PLA microspheres prepared in THF.

4. Conclusion

In summary, we have developed novel DOX-loaded stereocomplexed microparticles with controlled size and microstructure for use as drug delivery system in cancer therapy. This was done by applying different organic solvents, namely, THF, DIOX, and their binary mixtures and by tuning the PLA end group functionality, namely, Boc-protected L-proline versus unblocked L-proline PLAs. We systematically

screened different conditions and found that the smaller particles are obtained from unblocked L-proline PLAs, whereas their morphology is determined by the solvent from which these particles are prepared. Moreover, by tuning the preparation conditions we could modify the DOX loading and release efficiency. Interestingly, *in vitro* experiments in which we observed the highest efficiency for particles composed of L-proline PLAs which can deliver DOX in the fastest manner, correlates with their antiproliferative activity. Moreover, the size also determines their uptake by lung cancer cells. These advantageous features indicate that stereocomplexed microspheres can enhance the efficiency of chemotherapy against lung cancer as these DOX-loaded microcarriers could be potentially administrated to the lungs by inhalation.

Acknowledgements

M. Brzezinski and M. Socka acknowledges for support from the National Science Centre Poland Grant DEC-2016/23/D/ST5/02458. S. Wedepohl and M. Calderón gratefully acknowledge financial support from Bundesministerium für Bildung und Forschung (BMBF) through the NanoMatFutur award (13N12561) and IKERBASQUE-Basque Foundation for Science.

Appendix A. Supplementary data

Supplementary material related to this article can be found, in the online version, at doi:https://doi.org/10.1016/j.colsurfb.2019.110544.

References

[1] B. Tyler, D. Gullotti, A. Mangraviti, T. Utsuki, H. Brem, Polylactic acid (PLA) controlled delivery carriers for biomedical applications, Adv. Drug Deliv. Rev. 107 (2016) 163–175, https://doi.org/10.1016/j.addr.2016.06.018.
[2] A.C. Albertsson, I.K. Varma, Recent developments in ring opening polymerization of lactones for biomedical applications, Biomacromolecules. 4 (2003) 1466–1486, https://doi.org/10.1021/bm034247a.
[3] H. Seyednejad, A.H. Ghassemi, C.F. Van Nostrum, T. Vermonden, W.E. Hennink, Functional aliphatic polyesters for biomedical and pharmaceutical applications, J. Control, Release. 152 (2011) 168–176, https://doi.org/10.1016/j.jconrel.2010.12.016.
[4] H. Tsuji, Poly(lactide) stereocomplexes: Formation, structure, properties, degradation, and applications, Macromol. Biosci. 5 (2005) 569–597, https://doi.org/10.1002/mabi.200500062.
[5] K. Kan, M. Akashi, H. Ajiro, Polylactides bearing vanillin at chain end provided dual dynamic interactions: stereocomplex formation and nanostructure control, Macromol. Chem. Phys. 217 (2016) 2679–2685, https://doi.org/10.1002/macp.201600395.
[6] S. Fujishiro, K. Kan, M. Akashi, H. Ajiro, Stability of adhesive interfaces by stereocomplex formation of polylactides and hybridization with nanoparticles, Polym. Degrad. Stab. 141 (2017) 69–76, https://doi.org/10.1016/j.polymdegradstab.2017.05.010.
[7] H. Bai, S. Deng, D. Bai, Q. Zhang, Q. Fu, Recent advances in processing of stereocomplex-type polylactide, Macromol. Rapid Commun. 38 (2017) 1–12, https://doi.org/10.1002/marc.201700454.
[8] M. Brzeziński, T. Biela, Micro- and nanostructures of polylactide stereocomplexes and their biomedical applications, Polym. Int. 64 (2015) 1667–1675, https://doi.org/10.1002/pi.4961.
[9] Z. Li, B.H. Tan, T. Lin, C. He, Recent advances in stereocomplexation of enantiomeric PLA-based copolymers and applications, Prog. Polym. Sci. 62 (2016) 22–72, https://doi.org/10.1016/j.progpolymsci.2016.05.003.
[10] M. Socka, M. Brzezinski, A. Michalski, A. Kacprzak, T. Makowski, A. Duda, Self-assembly of triblock copolymers from cyclic esters as a tool for tuning their particle morphology, Langmuir 34 (2018) 3701–3710, https://doi.org/10.1021/acs.langmuir.8b00440.
[11] Z. Chen, Y. Chang, Z. Jiang, Facile fabrication of polylactic acid stereocomplex microspheres, Mater. Lett. 211 (2018) 146–148, https://doi.org/10.1016/j.matlet.2017.09.089.
[12] H. Tsuji, S.H. Hyon, Y. Ikada, Stereocomplex Formation between Enantiomeric Poly (lactic acid)s. 5. Calorimetric and Morphological Studies on the Stereocomplex Formed in Acetonitrile Solution, Macromolecules. 25 (1992) 2940–2946, https://doi.org/10.1021/ma00037a024.
[13] H. Tsuji, Poly(lactic acid) stereocomplexes: A decade of progress, Adv. Drug Deliv. Rev. 107 (2016) 97–135, https://doi.org/10.1016/j.addr.2016.04.017.
[14] B. Yu, L. Meng, S. Fu, Z. Zhao, Y. Liu, K. Wang, Q. Fu, Morphology and internal structure control over PLA microspheres by compounding PLLA and PDLA and effects on drug release behavior, Colloids Surf. B Biointerfaces 172 (2018) 105–112, https://doi.org/10.1016/j.colsurfb.2018.08.037.
[15] S. Boi, E. Dellacasa, P. Bianchini, P. Petrini, L. Pastorino, O. Monticelli, Encapsulated functionalized stereocomplex PLA particles: an effective system to support mucolytic enzymes, Colloids Surf. B Biointerfaces 179 (2019) 190–198, https://doi.org/10.1016/j.colsurfb.2019.03.071.
[16] S.H. Lee, T.C. Boire, J.B. Lee, M.K. Gupta, A.L. Zachman, R. Rath, H.J. Sung, ROS-cleavable proline oligomer crosslinking of polycaprolactone for pro-angiogenic host response, J. Mater. Chem. B Mater. Biol. Med. 2 (2014) 7109–7113, https://doi.org/10.1039/c4tb01094a.
[17] L. Gordon, Amidon Sachin Mittal, Xueqin Song, S.Vig Balvinder, 1, Proline prodrug of melphalan targeted to prolidase, a prodrug activating enzyme overexpressed in melanoma, Pharm. Res. 24 (2007) 1290–1298, https://doi.org/10.1007/s11095-007-9249-9.
[18] J. Farrera-Sinfreu, E. Giralt, S. Castel, F. Albericio, M. Royo, Cell-penetrating cis-γ-amino-L-proline-derived peptides, J. Am. Chem. Soc. 127 (2005) 9459–9468, https://doi.org/10.1021/ja051648k.
[19] J. Singh, R. Singh, P. Gupta, S. Rai, A. Ganesher, P. Badrinarayan, G.N. Sastry, R. Konwar, G. Panda, Targeting progesterone metabolism in breast cancer with L-proline derived new 14-azasteroids, Bioorg. Med. Chem. Lett. 25 (2017) 4452–4463, https://doi.org/10.1016/j.bmc.2017.06.031.
[20] F. Ito, H. Fujimori, H. Honnami, H. Kawakami, K. Kanamura, K. Makino, Study of types and mixture ratio of organic solvent used to dissolve polymers for preparation of drug-containing PLGA microspheres, Eur. Polym. J. 45 (2009) 658–667, https://doi.org/10.1016/j.eurpolymj.2008.12.037.
[21] A. Michalski, T. Makowski, T. Biedroń, M. Brzeziński, T. Biela, Controlling polylactide stereocomplex (sc-PLA) self-assembly: from microspheres to nanoparticles, Polymer (Guildf). 90 (2016) 242–248, https://doi.org/10.1016/j.polymer.2016.03.049.
[22] T. Biedroń, M. Brzeziński, T. Biela, P. Kubisa, Microspheres from stereocomplexes of polylactides containing ionic liquid end-groups, J. Polym. Sci. Part A: Polym. Chem. 50 (2012) 4538–4547, https://doi.org/10.1002/pola.26266.
[23] N. Naga, Y. Yoshida, K. Noguchi, Crystallization of poly(L-lactic acid)/poly(D-lactic acid) blend induced by organic solvents, Polym. Bull. 76 (2019) 3677, https://doi.org/10.1007/s00289-018-2563-z.
[24] A. Lu, T.P. Smart, T.H. Epps, D.A. Longbottom, R.K. O'Reilly, L-proline functionalized polymers prepared by RAFT polymerization and their assemblies as supported organocatalysts, Macromolecules. 44 (2011) 7233–7241, https://doi.org/10.1021/ma201256m.
[25] A. Kowalski, J. Libiszowski, T. Biela, M. Cypryk, A. Duda, S. Penczek, Kinetics and mechanism of cyclic esters polymerization initiated with tin(II) octoate. Polymerization of ε-caprolactone and L,L-Lactide co-initiated with primary amines, Macromolecules 38 (2005) 8170–8176, https://doi.org/10.1021/ma050752j.
[26] J.R. Sarasua, N.L. Rodriguez, A.L. Arraiza, E. Meaurio, Stereoselective crystallization and specific interactions in polylactides, Macromolecules. 38 (2005) 8362–8371, https://doi.org/10.1021/ma051266z.
[27] A. Michalski, M. Socka, M. Brzeziński, T. Biela, Reversible supramolecular polylactides gels obtained via Stereocomplexation, Macromol. Chem. Phys. (2018) 1700607, , https://doi.org/10.1002/macp.201700607.
[28] H. Mori, I. Kato, M. Matsuyama, T. Endo, RAFT polymerization of acrylamides containing proline and hydroxyproline moiety: controlled synthesis of water-soluble and thermoresponsive polymers, Macromolecules. 41 (2008) 5604–5615, https://doi.org/10.1021/ma800181h.
[29] H. Mori, I. Kato, S. Saito, T. Endo, Proline-based block copolymers displaying upper and lower critical solution temperatures, Macromolecules. 43 (2010) 1289–1298, https://doi.org/10.1021/ma902002b.
[30] T. Biela, A. Duda, S. Penczek, Enhanced melt stability of star-shaped stereocomplexes as compared with linear stereocomplexes, Macromolecules. 39 (2006) 3710–3713, https://doi.org/10.1021/ma060264r.
[31] M. Brzeziński, S. Wedepohl, B. Kost, M. Calderón, Nanoparticles from supramolecular polylactides overcome drug resistance of cancer cells, Eur. Polym. J. 109 (2018) 117–123, https://doi.org/10.1016/j.eurpolymj.2018.08.060.
[32] R. Lin, L.S. Ng, C.H. Wang, In vitro study of anticancer drug doxorubicin in PLGA-based microparticles, Biomaterials. 26 (2005) 4476–4485, https://doi.org/10.1016/j.biomaterials.2004.11.014.
[33] Q. Xu, Y. Xia, C.H. Wang, D.W. Pack, Monodisperse double-walled microspheres loaded with chitosan-p53 nanoparticles and doxorubicin for combined gene therapy and chemotherapy, J. Control, Release. 163 (2012) 130–135, https://doi.org/10.1016/j.jconrel.2012.08.032.
[34] J.H. Moon, S. Yang, Chemical aspects of three-dimensional photonic crystals, Chem. Rev. 110 (2010) 547–574, https://doi.org/10.1021/cr900080v.
[35] S.H. Kim, F. Nederberg, L. Zhang, C.G. Wade, R.M. Waymouth, J.L. Hedrick, Hierarchical Assembly of Nanostructured Organosilicate Networks via Stereocomplexation of Block Copolymers, Nano Lett. 81 (2008) 294–301.
[36] M. Brzeziński, T. Biedroń, A. Tracz, P. Kubisa, T. Biela, Spontaneous formation of colloidal crystals of PLA stereocomplex microspheres and their hierarchical structure, Macromol. Chem. Phys. 215 (2014) 27–31, https://doi.org/10.1002/macp.201300491.
[37] H.M. Yadav, N.D. Thorat, M.M. Yallapu, S.A.M. Tofail, J. Kim, Functional TiO2 nanocoral architecture for light-activated cancer chemotherapy, J. Mater. Chem. B (2017) 1461–1470, https://doi.org/10.1039/C6TB02324J.
[38] M.P. Deasi, V. Labhasetwar, E. Walter, R.J. Levy, G.L. Amidon, The mechanism of uptake of biodegradable microparticles in Caco-2 cells is size dependent, Pharm. Res. 14 (1997) 1568–1573.